

IGDrivSim: A Benchmark for the Imitation Gap in Autonomous Driving

Clémence Grislain

Sorbonne University*
clemgris@gmail.com

Risto Vuorio

University of Oxford

Cong Lu

University of British
Columbia Vector Institute

Shimon Whiteson

University of Oxford

Abstract—Developing autonomous vehicles that can navigate complex environments with human-level safety and efficiency is a central goal in self-driving research. A common approach to achieving this is imitation learning, where agents are trained to mimic human expert demonstrations collected from real-world driving scenarios. However, discrepancies between human perception and the self-driving car’s sensors can introduce an *imitation gap*, leading to imitation learning failures. In this work, we introduce IGDrivSim, a benchmark built on top of the Waymax simulator, designed to investigate the effects of the imitation gap in learning autonomous driving policy from human expert demonstrations. Our experiments show that this perception gap between human experts and self-driving agents can hinder the learning of safe and effective driving behaviors. We further show that combining imitation with reinforcement learning, using a simple penalty reward for prohibited behaviors, effectively mitigates these failures. Our code is open-sourced at: <https://github.com/clemgris/IGDrivSim.git>.

I. INTRODUCTION

Research in autonomous driving aims to develop vehicles capable of navigating complex environments with the safety and efficiency of human drivers [1], [2]. Learning such autonomous driving policies has been a focus of the research community due to its potential to reduce transportation costs, alleviate labor constraints, improve road safety, and enhance overall mobility [3]. However, achieving this level of performance remains a critical challenge in the field. In fact, while reinforcement learning (RL, [4]) has been a natural solution for control in various domains such as robotics and game playing [5], self-driving agents often struggle to learn desired behaviors using RL due to the high computational cost and, more critically, the difficulty of designing an effective reward function. In these scenarios, imitation learning from human driver demonstrations (IL, [6], [7]) is a popular alternative for training policies. IL allows self-driving agents to learn directly from human expert behaviors, bypassing the need for an explicit reward function and reducing computational costs. In the literature, expert datasets often consist of traffic scenarios where multiple road users are tracked in 3D space using sensors from a human-driven car [8], [9], [10]. These data are relatively simple to record in real-world environments, and training typically involves simulators that replicate these recorded driving scenarios, with the task being to predict the trajectories of each agent throughout the scene.

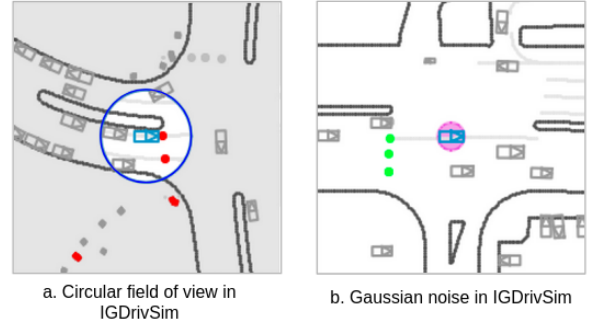


Fig. 1: Screenshots of two scenarios in IGDrivSim illustrating the introduction of partial observability. The controlled vehicle, shown in blue, navigates among road lines, street lights, and other vehicles. On the left, an agent with a circular field of view is depicted, with its visibility limited by blue boundaries, while gray-shaded regions represent occluded information. On the right, an agent experiences noisy position perception of its position within the scene, visualized by the magenta-shaded area.

However, a major challenge of IL arises when the imitator and the expert have different *observability* of the environment, which can occur, for instance, when they rely on different sensors. This difference can lead to an *imitation gap* [11], [12], [13], [14] and potentially cause IL algorithms to fail. Imagine training an autonomous vehicle to navigate in a foggy area by imitating data from another vehicle that was recorded in clear weather. The expert vehicle, operating in clear conditions, can see far ahead and navigate smoothly, anticipating obstacles and changes in the environment well in advance. However, when the imitator behaves in an area with dense fog, it cannot see as far ahead and must rely solely on its limited visibility to navigate. If the imitator simply copies the expert’s actions, driving at the same speed and making the same turns, it will likely fail because it does not have the same information about the road ahead. Instead, a better policy for the imitator would involve slowing down and adopting a less smooth but more reactive behavior to avoid obstacles. This cautious and adaptive behavior allows the imitator to compensate for its reduced visibility and safely navigate through foggy conditions. However, this behavior is never demonstrated by the expert vehicle and therefore not learned by the imitator.

In this example, the difference in observability between the expert and the imitator would cause traditional IL algorithms to fail. Critically, the common practice of training au-

*Work done while interning at University of Oxford

Autonomous driving policies using simulators based on human driver trajectories naturally introduces a similar difference in observability between the human expert and the self-driving car (SDC), which could likewise result in the failure of IL. In fact, when performing IL, the SDC has access to all the information recorded during data collection, typically involving sensors like LiDAR and cameras. Yet, these sensors differ in their capabilities from human perception, on which the human driver relies to generate expert demonstrations. For example, a human driver might react based on audio cues like honks that the SDC might not detect if it lacks audio sensors. Conversely, human drivers might not see certain information due to visual blind spots that the SDC would detect with its broader field of view. These differences in the perception of the driving environment between the human expert and the SDC imitator create an imitation gap. Imitation learning from the human expert demonstrations may lead to the SDC imitator not learning the specific behaviors required for its particular sensory capabilities (i.e., the sensors used to collect scene information). In the best case, the learned policy is safe but suboptimal under the SDC’s observability; in the worst case, it learns unsafe behaviors. While the imitation gap has been studied in previous work [12], [13], [14], to our knowledge, there exists no dedicated benchmark for evaluating how this difference in observability affects the learning of driving policies from human demonstrations.

Therefore, we introduce **IGDrivSim** (Imitation Gap in Driving Simulation), a benchmark specifically designed to explore the impact of the imitation gap on learning driving policies from human demonstrations. IGDrivSim introduces constraints (see Figure 1) on the observability of the Waymax driving simulator [15], which is based on the WOMD dataset [10] of real-world human driving data. These constraints amplify the difference between the human expert’s and the simulated self-driving car’s observability, effectively widening the imitation gap. Our experiments reveal that when trained with IL, especially behavioral cloning, a self-driving agent—whose observations of the driving scene inherently differ from human perception—struggles to learn good behaviors from human expert demonstrations alone and that this failure can be explained by the presence of an imitation gap. Furthermore, we demonstrate that incorporating knowledge about prohibited behaviors can help address this issue. In fact, we find that by combining IL with RL based on a simple penalty reward, we can mitigate these failures. While [16] demonstrated that reward signals can enhance IL, the underlying reasons were not fully explored. In this work, we present a novel setup and results that, for the first time, show how an imitation gap can explain the need for supplemental methods like RL in training self-driving policies with IL. By introducing IGDrivSim as a benchmark, we aim to provide a tool for evaluating and addressing the imitation gap in autonomous driving, facilitating both the assessment and improvement of IL from human driving demonstrations.

In summary, the contributions of our work are:

- 1) We release an open-source benchmark, called IG-

DrivSim, for studying the imitation gap in a high-dimensional, real-world complex task where IL is the current state-of-the-art method for training policies.

- 2) We underscore the importance of addressing the imitation gap when training self-driving car policies on human driver data, revealing key limitations of demonstration-based IL.
- 3) We release the first (to our knowledge) open-source motion prediction baselines, which are based on a simple RNN architecture, trained on the Jax-based simulator Waymax.

II. BACKGROUND

A. Preliminaries

a) Reinforcement Learning: We define the environment as a Partially Observable Markov Decision Process (POMDP) [17], characterized by the tuple $\mathcal{M} := \langle \mathcal{S}, \mathcal{A}, p(s_{t+1}|s_t, a_t), r(s_t, a_t), \Omega, O(s_t), \gamma \rangle$. Similar to the classic MDP definition, \mathcal{S} and \mathcal{A} denote the state and action spaces respectively, $p(s_{t+1}|s_t, a_t)$ represents the transition dynamics, and $r(s_t, a_t)$ is the reward function. However, in a POMDP, the agent observes the environment through an observation function $O : \mathcal{S} \rightarrow \mathcal{P}(\Omega)$, which maps states to probability distributions over the observation space Ω . In RL, the objective is to optimize a policy $\pi(a|z)$ with $z \sim O(s)$ that maximizes the expected return $\mathbb{E}_{\pi, p} [\sum_{t=0}^{\infty} \gamma^t r(s_t, a_t)]$.

b) Behavioral Cloning: In imitation learning, we assume access to a set of expert demonstrations $\mathcal{D}_{\text{expert}} := \{\tau_i\}_{i=1}^{N_{\text{expert}}}$ of state-action trajectories $\tau_i = \{s_0, a_0, s_1, a_1, \dots\}$ from which an imitator learns a behavior. Behavioral cloning (BC, [18]) is an IL method where the objective is to learn a policy $\pi(a|z)$ with $z \sim O(s)$ that maximizes the negative log-likelihood of the expert actions with respect to the action distribution predicted by the imitator along the expert’s trajectory $\sum_{\tau_i \in \mathcal{D}_{\text{expert}}} \log \pi(a_i|z_i)$ with $z_i \sim O(s_i)$.

c) Imitation Gap Problem: An imitation gap arises when the demonstrator and the imitator have different observation functions, i.e., $O_{\text{expert}} \neq O_{\text{imitator}}$. A sufficient condition for the imitation gap to cause IL failure (i.e., leading to a suboptimal policy as described in [11]) is when the expert’s policy, which generates the expert demonstrations, becomes suboptimal in the imitator’s POMDP. In other words, the expert’s policy, which is assumed to be Bayes-optimal [19] in the expert’s POMDP, is no longer Bayes-optimal in the imitator’s POMDP, due to the imitation gap.

As a result, the imitator might need to deviate from the expert to learn an optimal policy in its own POMDP. However, standard demonstration-based IL algorithms do not allow such deviations. For instance, BC minimizes the discrepancy between the expert’s and the imitator’s state-action pairs, while Generative Adversarial Imitation Learning (GAIL, [20]) additionally maximizes the discrepancy between non-expert and imitator state-action pairs. In both approaches, the imitator is still constrained to closely follow the expert’s behavior. Therefore, although this work uses BC to illustrate IL failures under the imitation gap, GAIL will

also encounter similar issues, as shown in [12] in simpler environments. To address the imitation gap and enable the imitator to learn an optimal policy, additional guidance is required. This can be provided through an explicit Bayesian prior [14], which leverages prior knowledge, or through the environment’s reward signal [12], which can help align the imitator’s learning process with optimal behavior.

B. Waymax Simulator

Waymax is a Jax-based data-driven simulator built on the WOMB dataset, which consists of trajectories of cars, other road users, and road features recorded in diverse urban driving scenarios. The WOMB dataset contains more than 570 hours of data collected over 1,750 km of roadways across six United States cities. The data consists of 9.1 seconds of driving scenario mined for extracting interactive behaviors from 20-second initial segments. Sampled at 10Hz, each scenario is divided into 91 timesteps, with the first 10 timesteps serving as context and the remaining 81 used for behavior prediction. The task is to predict the future trajectories of the vehicles in each scenario.

C. Action Space

The Waymax simulator introduces a *delta* car control model, where the action space is continuous and defined by the position and yaw displacements $(\Delta x, \Delta y, \Delta \theta)$ of the agent between two consecutive states. When an agent in position and yaw (x, y, θ) takes action $(\Delta x, \Delta y, \Delta \theta)$ it transitions to $(x + \Delta x, y + \Delta y, \theta + \Delta \theta)$. Its speed is also updated to $v_x = \Delta x / \Delta t$ and $v_y = \Delta y / \Delta t$. This action space is advantageous as the inverse kinematics used to derive the expert’s actions from the logged trajectory, required for BC in particular, are straightforward.

D. State Space

The Waymax state space is composed of map data and information about the objects in the scene. Following [21], map data are provided as a set of polylines created from curves sampled at a resolution of 0.5 meters. Polyline points are characterized by road feature types (lane centers, lane boundary lines, road edges, stop signs, crosswalks, and speed bumps). Objects are represented as bounding boxes (3D center point, heading, length, width, and height), and velocity vectors [10]. The imitator learns from the trajectory of the ego car, perceiving the scene from its viewpoint after projecting the entire scene (objects and road map) from the global frame of reference to the ego car’s local frame. We limit the information about scene objects to the tuple (x, y, z, v, yaw) which includes their positions $(x, y, z) \in \mathbb{R}^3$, velocity $v \in \mathbb{R}_+$, and heading $yaw \in [0, 2\pi]$.

III. HIGHLIGHTING AND MITIGATING THE IMITATION GAP

A. Imitation Learning Failure under the Imitation Gap

To provide insight into why IL can fail in the presence and imitation gap, we examine a simple navigation problem where an agent has to reach a goal within a maze in the

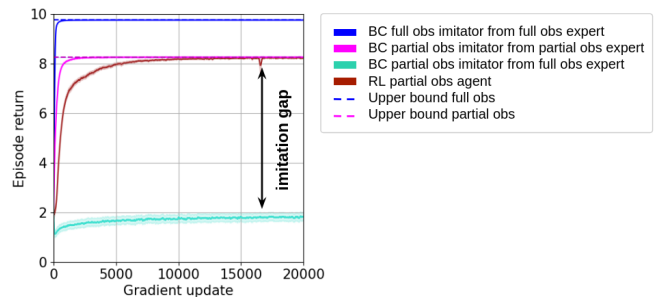


Fig. 2: The solid lines show episodic returns during the training of agents with full or partial observability (receptive field size of 3), trained using RL or BC from demonstrations generated by experts with corresponding observability. Dashed lines indicate approximate upper bound returns, computed as mean returns of converged agents trained with RL under full and partial observability (receptive field size of 3) which approximate Bayes-optimal policies. Shading represents the mean and 95% confidence interval across 10 seeds.

fewest possible timesteps. In this environment, we define two POMDPs for the expert and the imitator, differing in their observation functions. The imitator’s observation function, defined by the agent’s receptive field, masks the goal’s position when it falls outside its field, whereas the expert always accesses the goal position.

In this setting, the expert demonstrates only goal-directed behaviors. However, for the imitator to solve the task, the optimal policy requires exploring the environment to locate the goal first. When trained on demonstrations generated by the expert with full observability, the imitator will never learn the necessary exploration behavior, resulting in a suboptimal policy under the imitator’s POMDP. To characterize this failure, we approximate the Bayes-optimal policy for the imitator’s POMDP using PPO [22] and show that this policy cannot be achieved by training the imitator with BC on demonstrations from an expert with full observability of the goal’s position.

Figure 2 presents the results of this experiment in a 13×13 maze with a receptive field size of 3 for the imitator. The results indicate that the imitator with partial observability, trained on demonstrations from the expert with full observability (in turquoise), cannot learn an optimal policy w.r.t. its observability, and achieves suboptimal returns. On the other hand, when the expert and imitator share the same level of observability—either full or partial with a receptive field size of 3 (respectively in blue and magenta)—the imitator quickly learns an optimal policy with BC and achieves the maximum return. While in this environment the ground truth reward is known, which allows an optimal policy to be learned through RL (in brown), in many real-world scenarios, like autonomous driving, such reward fully defining the desired behavior is often inaccessible. Therefore, learning policy relies heavily on IL, hence the importance of addressing the imitation gap.

B. Mitigating the Imitation Gap Problem with RL

The failure of IL under mismatched expert and imitator observabilities occurs because the expert demonstrates be-

haviors that are optimal for the expert’s POMDP but not for the imitator’s POMDP. Consequently, for the imitator to learn behaviors optimal for its own partial observability, it must rely on signals outside the expert demonstration dataset. Although IL is typically employed in environments where defining a reward function for training a good policy is impractical, it is often possible to access a reward function that penalizes undesirable behaviors, such as safety metrics in autonomous driving.

While this reward may not fully characterize the desired behavior, and training solely based on it is impractical, it can still be used as an additional signal. This idea has been exploited by previous work [12] as a solution for mitigating the imitation gap problem. Following a similar approach to [16], we introduce a combined loss that leverages BC to learn generally useful behaviors from the expert and RL to learn behaviors specific to the imitator’s observability. Here, the RL loss acts as a regularizer for the BC loss:

$$\mathcal{L}(\phi) = \omega_{BC} \mathcal{L}_{BC}(\phi, \mathcal{D}_{\text{expert}}) + \omega_{RL} \mathcal{L}_{RL}(\phi), \quad (1)$$

where ϕ represents the parameters of the imitator policy, and $(\omega_{BC}, \omega_{RL})$ are two hyperparameters. The BC loss is the negative log-likelihood of the expert’s actions with respect to the action distribution predicted by the imitator policy, as defined in Section II-A. While we use BC loss, other standard IL algorithms and their respective loss functions can be used. The RL loss can also be derived from any RL algorithm; in this work, we use PPO [22].

C. Highlighting the Imitation Gap in Waymax

To highlight the imitation gap problem, we introduce IGD_{Drive}Sim, which incorporates imitators with partial observability of the road and surrounding vehicles into the original Waymax simulator. In practice, IGD_{Drive}Sim considers observation functions that act as a mask, obscuring the features of cars and road points outside a particular region. For this work, we consider a circular region characterized by a radius $r \in \mathbb{R}_+$, as shown in Figure 1. Additionally, IGD_{Drive}Sim considers another form of partial observability by introducing noise into the perception of the Waymax scenario features. Specifically, it applies Gaussian noise to the position of the ego car in the global frame of reference, with zero mean and a standard deviation of σ . This noise remains constant throughout the entire trajectory. Since the SDC’s observations are projected into the ego referential frame, this is equivalent to adding a constant noise to the positions of all other cars as well as the road points. These agents with partial observability can be seen as self-driving agents operating in environments with extreme conditions that limit their vision of the road and of the other cars, similar to the scenarios described in the introduction, or to self-driving vehicles with noisy sensors. Due to computational constraints, the experiments were limited to these two types of partial observability. However, IGD_{Drive}Sim offers a broader range of partial observability constraints, including conic and blind spot fields of view, random masking, and observability that varies with the agent’s speed.

D. Metrics

To evaluate the imitator’s driving policy, we rely on safety metrics as well as metrics characterizing how far the imitator’s behavior deviates from the expert’s. We use the timestep metrics introduced in Waymax: *overlap* (a binary metric indicating if the controlled agent is overlapping and therefore colliding with another vehicle), *off-road* (a binary metric indicating if the controlled agent drives off the road), and *log divergence* (measuring how far the position of the controlled agent deviates from the expert’s position). We also extended these metrics to encompass the entire scenario, introducing the *overlap rate* (a binary metric indicating if the controlled agent collides at least once during the scenario), the *off-road rate* (a binary metric indicating if the controlled agent drives off the road at least once during the scenario) and the *maximal log divergence* along the entire trajectory.

E. Reward

To compute the RL component of the combined loss defined in Equation 1, we utilize the reward function defined in the Waymax simulator, which is the sum of safety penalties incurred during each time step, specifically due to off-road driving and vehicle overlap:

$$r_t = -\mathbb{1}_{\text{overlap}}(t) - \mathbb{1}_{\text{off-road}}(t),$$

where $\mathbb{1}_{\text{overlap}}(t)$ is an indicator function that equals one if the ego vehicle collides with another vehicle at timestep t , and $\mathbb{1}_{\text{off-road}}(t)$ equals one if the ego vehicle is driving off the road at timestep t .

IV. EXPERIMENTS

Our experiments reveal BC’s limitations when used to train driving policies from human demonstrations, and establish IGD_{Drive}Sim as a valuable benchmark for addressing imitation gaps between human drivers and self-driving agents.

A. Training

a) Architecture: When training agents with BC, we use two different encoders to embed the scene observations: an MLP for encoding the objects’ features and a polyline encoder, based on the architecture proposed in [23], for the roadgraph. We apply layer norms on the two embeddings, which are then concatenated and passed to a simple recurrent neural network (RNN) with a final softmax layer to compute action probabilities. Supported by the results of [15], we discretize the action space into 256 bins. The RNN enables handling the partial observability in the environment by maintaining and updating a hidden state that captures information about the environment over time despite limited observations at each timestep. For RL, we used the same architecture but added an MLP value head after the RNN cell.

b) Policy Update: During training with the combined BC and RL loss, we consider two types of trajectories for each scenario: a logged trajectory, where the simulator is updated using the expert’s actions, and a simulated trajectory, where the simulator is updated using the imitator’s actions. The BC component is calculated by computing the negative log-likelihood of the expert’s actions based on the action distribution predicted by the imitator policy over the entire logged trajectory. Furthermore, to reduce distribution shift, we follow a similar approach to [24] by discretizing the expert’s demonstrations using the expert agent introduced in Waymax. The scenario is then reset, and the imitator policy is used to generate a new trajectory, with rewards recorded at each timestep. The RL component, represented by the PPO loss, is computed on this imitator-driven trajectory. Finally, the model is updated using the Adam optimizer with a cosine decay learning rate, ranging from 10^{-3} to 0, applied to the combined loss as defined in Equation 1. Each training run took approximately 2 days on a cluster of 8 NVIDIA GTX 1080 GPUs.

c) Training Set: We filter the WOMB training dataset, which initially contained 487,002 driving scenarios, to retain only those where the ego car demonstrates interactive behavior. A scenario is classified as interactive if the ego car’s trajectory intersects with another object’s trajectory during the scenario. This reduces the training dataset by approximately 50%. To further reduce the dataset, we exclude scenarios where the ego car’s mean speed throughout the trajectory is less than 0.7 m/s. The final dataset consists of 152,808 scenarios, representing approximately 31% of the original WOMB training set.

d) Test Set: As the logged trajectories of the WOMB test set have not been released, we evaluate the performances of our trained policies on the validation set, distinct from the training set, which is composed of 44,097 driving scenarios.

B. Results

To demonstrate that under imitation gaps—widened in IGDrivSim by artificial constraints on the imitator’s observability—BC alone fails to learn efficient and safe behavior for the imitator’s specific observability, we train imitators with varying observability. We then compare the policies learned through BC on human expert demonstrations with those trained using a combined BC and RL loss. As our focus is on IL of a single agent; while Waymax allows for controlling all the agents of the scene, we restrict the control to the ego car from which the scene was recorded.

In the toy environment, we access a reward function that fully defines the desired behavior, allowing us to approximate the Bayes-optimal policy and thus characterize BC failure as the performance gap between the BC policy and the approximate Bayes-optimal policy under the imitator’s POMDP. However, in the Waymax environment, such a reward function is inaccessible. Instead, by using the BC-RL combined loss, we show that there exists a superior policy under the imitator’s POMDP that BC alone fails to recover. This approach establishes a lower bound on the performance

gap between the BC policy and the Bayes-optimal policy in the presence of the imitation gap.

We evaluate four imitators: one with full observability using the initial Waymax settings, two with circular fields of view in IGDrivSim with radii of 4 meters and 6 meters, and one operating under Gaussian noise in IGDrivSim with a standard deviation of 3 meters, as defined in section III-C. These agents’ perceptions differ significantly from human expert perception, thereby introducing an imitation gap in the training process. Notably, even the agent with full observability relies solely on sensor-recorded data, which inherently diverges from true human perception that could include additional factors such as traffic sounds. Our preliminary experiments show that for the observability constraints to impact performance compared to full observability, the radius must be narrow enough to limit the agent’s view of its immediate surroundings and the noise to be strong enough to introduce uncertainty. These restrictions prevent the agent from anticipating changes in the environment and forces it to learn a different policy compared to when it has access to the entire Waymax state, thereby introducing varying degrees of imitation gap.

Table I provides detailed values for the trajectory and per-step metrics—log divergence, overlap, and off-road—while Figure 3 shows a comparison of the per-step metrics, for policies trained with BC and the combined BC-RL loss across the four considered imitators. For all the imitators, balancing the BC loss with the RL loss using the simple penalty reward helps the agent learn a safer policy, reducing both overlap and off-road incidents. This demonstrates that using the BC-RL combined loss allows for better behavior learning under the imitator’s POMDP than BC alone. Although [16] highlights similar findings, they do not address the imitation gap, which we consider a key factor in explaining these results. Moreover, unlike [16], we have open-sourced our code, making these findings more accessible to the research community.

Interestingly, among the imitators with full observability, Gaussian noise, and a circular field of view with a radius of 6, the policy learned with the combined loss not only minimizes safety metrics but also exhibits better log divergence—meaning it is closer to the expert’s policy—than the policy trained only with BC. By contrast, the imitator with a circular field of view of radius 4, also trained with the combined loss, shows higher log divergence than the BC policy, despite improvements in overlap and off-road incidents. This indicates that the policy trained with the combined loss diverges from the expert’s but performs better within its own POMDP. By learning behaviors not demonstrated by the human expert, it effectively reduces overlap and off-road incidents based on its specific perception of the cars and road environment. This result highlights how RL regularization can allow learning optimal behaviors not shown in expert demonstrations, thus mitigating the imitation gap.

Qualitatively, the agent trained with the BC-RL combined loss shows greater reactivity to changes in its receptive field. For instance, it engages in heavy braking when the road

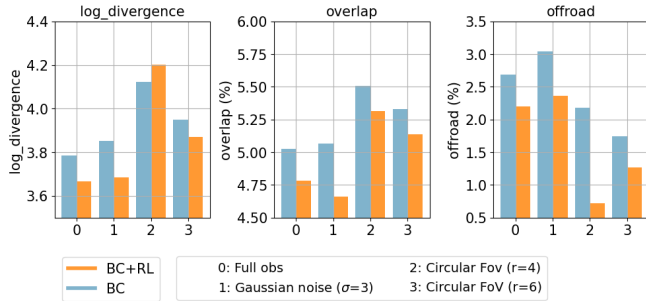


Fig. 3: Comparison of per-step metrics—log divergence, off-road, and overlap—between policies trained with BC (blue) and the combined BC-RL (BC+RL, orange) using parameters ($w_{BC} = 1, w_{RL} = 0.05$). The metrics are averaged over two seeds for four imitators defined by different partial observability in IGDriVSim.

TABLE I: Mean trajectory and per-step metrics for policies trained with BC and the combined BC-RL loss under different partial observability in IGDriVSim. Blue cells represent BC-only policies, while orange cells indicate BC-RL policies ($w_{BC} = 1, w_{RL} = 0.05$). All values are averaged over two seeds.

Metric	Full obs	Gaussian noise ($\sigma=3$)	Circular Fov ($r=4$)	Circular FoV ($r=6$)
log divergence	3.67	3.69	4.20	3.87
max log divergence	10.56	10.72	12.64	11.51
overlap (%)	4.78	4.66	5.32	5.14
overlap rate (%)	21.18	20.91	24.45	22.97
offroad (%)	2.20	2.36	0.72	1.26
offroad rate (%)	6.87	7.20	4.16	5.01

lines of other vehicles enter its view. In contrast, in several manually inspected scenarios, expert human drivers, having broader perception, anticipate road limits and nearby vehicles earlier, leading to smoother, more controlled braking and overall fluid driving behavior. The RL regularization of the BC loss enables the agent to learn behaviors that are effective within the imitator’s POMDP but not observed in the expert demonstrations. As a result, as shown in Figure 4, the self-driving car follows trajectories that diverge significantly from the expert-logged paths while remaining safe and efficient.

V. RELATED WORK

A variety of methods have been proposed recently to solve the imitation gap, but a lack of standardized benchmarks makes comparison among the algorithms harder. We provide a principled imitation gap benchmark with real-world motivation from learning policies for self-driving cars. A popular category of algorithms for solving the imitation gap combines BC and RL objectives using different weighting schemes. Weihs et al. [12] propose an algorithm that dynamically weights the objectives during training, while Nguyen et al. [25] start from an offline RL algorithm accelerated by

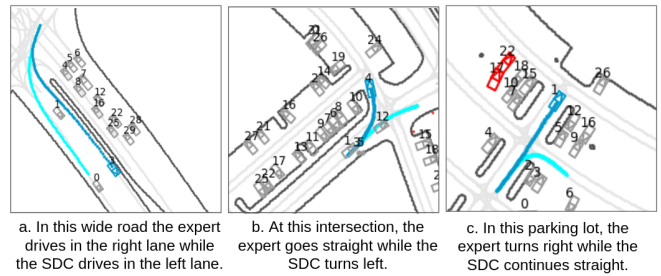


Fig. 4: Three examples showing the imitator (with a circular receptive field of radius 4) trained with the combined BC-RL loss, following distinct paths (in blue) compared to the human expert’s trajectories (in cyan).

the BC objective. Another solution idea is to use DAgger-style [26] online supervision to accelerate learning in an imitation gap setting [13]. Perhaps most closely related to ours is “Learning by Cheating” by Chen et al. [27], where they consider a vision-based driving setting with an imitation gap problem based on the CARLA driving simulator [8]. Vuorio et al. [14] show that prior information about the desired behaviors is always required to solve the imitation gap and propose a Bayesian solution to the problem. The failure of BC in problems with an imitation gap can be seen as a form of causal confounding [28]. When the imitator can solve the problem without deviating from the expert behavior, Ortega et al. [28] and Swamy et al. [29] show that DAgger-style methods can work well in this setting, while Vuorio et al. [30] use a separate inference model.

Learning driving policies is a popular field of research with multiple datasets and benchmarks targeting it. Waymo Open Dataset (WOMD) [10] contains many driving scenarios with log trajectories of human drivers. The Waymax [15] simulator we build upon runs on the scenarios from the WOMD dataset. Argoverse2 [31] provides an alternative to WOMD, while NuPlan [32] is one for Waymax. We chose Waymax due to its fast accelerator-compatible implementation and the large quantity of high-quality data included in WOMD. A closely related benchmark to ours is [33], which builds on WOMD and features partial observability. However, the effect of partial observability in Nocturne is unknown as it is not ablated.

BC is a popular method for learning driving policies. Seff et al. [24] propose to train a transformer policy on WOMD using BC. Lu et al. [16] demonstrate that BC is not always enough and show that combining BC with RL can improve metrics on the WOMD data. The current leader on the Waymo Open Sim Agents Challenge [34], which also uses WOMD data is also a transformer policy trained with BC [35].

VI. CONCLUSION

Our work highlights the challenges of training self-driving agents from human demonstrations when an imitation gap exists caused by differences in perception between human experts and self-driving car imitators. We introduce IGDriVSim, a benchmark designed to study how this gap affects IL from

human expert demonstrations. Our results show that self-driving cars trained only with IL often struggle to learn safe and efficient driving behaviors under their own perception of the environment when there is a significant imitation gap. However, we also found that combining IL with RL—using simple penalties for dangerous driving behaviors—can help mitigate these issues and improve overall performance. We release open-source code and motion prediction baselines trained on the Waymax simulator, for which no previous open-source baselines were available. We hope that IG-DrivSim will enhance understanding of IL from human driving demonstrations and lead to the development of safer and more effective self-driving policies tailored to the specific sensors of self-driving cars.

REFERENCES

- [1] J. Levinson, J. Askeland, J. Becker, J. Dolson, D. Held, S. Kammel, J. Z. Kolter, D. Langer, O. Pink, V. Pratt, M. Sokolsky, G. Stanek, D. Stavens, A. Teichman, M. Werling, and S. Thrun, "Towards fully autonomous driving: Systems and algorithms," in *2011 IEEE Intelligent Vehicles Symposium (IV)*, 2011, pp. 163–168.
- [2] E. Yurtsever, J. Lambert, A. Carballo, and K. Takeda, "A survey of autonomous driving: Common practices and emerging technologies," *IEEE Access*, vol. 8, pp. 58 443–58 469, 2020.
- [3] M. Maurer, J. C. Gerdes, B. Lenz, and H. Winner, *Autonomous driving: technical, legal and social aspects*. Springer Nature, 2016.
- [4] R. S. Sutton, "Reinforcement learning: An introduction," *A Bradford Book*, 2018.
- [5] V. Mnih, "Playing atari with deep reinforcement learning," *arXiv preprint arXiv:1312.5602*, 2013.
- [6] S. Schaal, "Is imitation learning the route to humanoid robots?" *Trends in Cognitive Sciences*, vol. 3, no. 6, pp. 233–242, 1999. [Online]. Available: <https://www.sciencedirect.com/science/article/pii/S1364661399013273>
- [7] A. Hussein, M. M. Gaber, E. Elyan, and C. Jayne, "Imitation learning: A survey of learning methods," *ACM Computing Surveys (CSUR)*, vol. 50, no. 2, pp. 1–35, 2017.
- [8] A. Dosovitskiy, G. Ros, F. Codevilla, A. Lopez, and V. Koltun, "Carla: An open urban driving simulator," 2017. [Online]. Available: <https://arxiv.org/abs/1711.03938>
- [9] A. Amini, T.-H. Wang, I. Gilitschenski, W. Schwarting, Z. Liu, S. Han, S. Karaman, and D. Rus, "Vista 2.0: An open, data-driven simulator for multimodal sensing and policy learning for autonomous vehicles," 2021. [Online]. Available: <https://arxiv.org/abs/2111.12083>
- [10] S. Ettinger, S. Cheng, B. Caine, C. Liu, H. Zhao, S. Pradhan, Y. Chai, B. Sapp, C. Qi, Y. Zhou, Z. Yang, A. Chouard, P. Sun, J. Ngiam, V. Vasudevan, A. McCauley, J. Shlens, and D. Anguelov, "Large scale interactive motion forecasting for autonomous driving : The waymo open motion dataset," 2021. [Online]. Available: <https://arxiv.org/abs/2104.10133>
- [11] G. Swamy, S. Choudhury, J. A. Bagnell, and Z. S. Wu, "Of moments and matching: A game-theoretic framework for closing the imitation gap," 2021. [Online]. Available: <https://arxiv.org/abs/2103.03236>
- [12] L. Weihs, U. Jain, I.-J. Liu, J. Salvador, S. Lazechnik, A. Kembhavi, and A. Schwing, "Bridging the imitation gap by adaptive insubordination," 2021. [Online]. Available: <https://arxiv.org/abs/2007.12173>
- [13] A. Walsman, M. Zhang, S. Choudhury, D. Fox, and A. Farhadi, "Impossibly good experts and how to follow them," in *The Eleventh International Conference on Learning Representations*, 2023. [Online]. Available: https://openreview.net/forum?id=sciA_xgYofB
- [14] R. Vuorio, M. Fellows, C. Lu, C. Grislain, and S. Whiteson, "A bayesian solution to the imitation gap," 2024. [Online]. Available: <https://arxiv.org/abs/2407.00495>
- [15] C. Gulino, J. Fu, W. Luo, G. Tucker, E. Bronstein, Y. Lu, J. Harb, X. Pan, Y. Wang, X. Chen, J. D. Co-Reyes, R. Agarwal, R. Roelofs, Y. Lu, N. Montali, P. Mouglin, Z. Yang, B. White, A. Faust, R. McAllister, D. Anguelov, and B. Sapp, "Waymax: An accelerated, data-driven simulator for large-scale autonomous driving research," 2023. [Online]. Available: <https://arxiv.org/abs/2310.08710>
- [16] Y. Lu, J. Fu, G. Tucker, X. Pan, E. Bronstein, R. Roelofs, B. Sapp, B. White, A. Faust, S. Whiteson, D. Anguelov, and S. Levine, "Imitation is not enough: Robustifying imitation with reinforcement learning for challenging driving scenarios," 2023. [Online]. Available: <https://arxiv.org/abs/2212.11419>
- [17] M. T. Spaan, "Partially observable markov decision processes," in *Reinforcement learning: State-of-the-art*. Springer, 2012, pp. 387–414.
- [18] D. A. Pomerleau, "Alvinn: An autonomous land vehicle in a neural network," in *Advances in Neural Information Processing Systems*, D. Touretzky, Ed., vol. 1. Morgan-Kaufmann, 1988. [Online]. Available: https://proceedings.neurips.cc/paper_files/paper/1988/file/812b4ba287f5ee0bc9d43bbf5bbe87fb-Paper.pdf
- [19] S. Ross, B. Chaib-draa, and J. Pineau, "Bayes-adaptive pomdps," in *Advances in Neural Information Processing Systems*, J. Platt, D. Koller, Y. Singer, and S. Roweis, Eds., vol. 20. Curran Associates, Inc., 2007. [Online]. Available: https://proceedings.neurips.cc/paper_files/paper/2007/file/3b3dbaf68507998acd6a5a5254ab2d76-Paper.pdf
- [20] J. Ho and S. Ermon, "Generative adversarial imitation learning," in *Advances in Neural Information Processing Systems*, D. Lee, M. Sugiyama, U. Luxburg, I. Guyon, and R. Garnett, Eds., vol. 29. Curran Associates, Inc., 2016. [Online]. Available: https://proceedings.neurips.cc/paper_files/paper/2016/file/cc7e2b878868cbac992d1fb743995d8f-Paper.pdf
- [21] J. Gao, C. Sun, H. Zhao, Y. Shen, D. Anguelov, C. Li, and C. Schmid, "Vectornet: Encoding hd maps and agent dynamics from vectorized representation," 2020. [Online]. Available: <https://arxiv.org/abs/2005.04259>
- [22] J. Schulman, F. Wolski, P. Dhariwal, A. Radford, and O. Klimov, "Proximal policy optimization algorithms," 2017. [Online]. Available: <https://arxiv.org/abs/1707.06347>
- [23] S. Shi, L. Jiang, D. Dai, and B. Schiele, "Motion transformer with global intention localization and local movement refinement," 2023. [Online]. Available: <https://arxiv.org/abs/2209.13508>
- [24] A. Seff, B. Cera, D. Chen, M. Ng, A. Zhou, N. Nayakanti, K. S. Refaat, R. Al-Rfou, and B. Sapp, "Motionlm: Multi-agent motion forecasting as language modeling," 2023. [Online]. Available: <https://arxiv.org/abs/2309.16534>
- [25] H. H. Nguyen, A. Baisero, D. Wang, C. Amato, and R. Platt, "Leveraging fully observable policies for learning under partial observability," in *6th Annual Conference on Robot Learning*, 2022.
- [26] S. Ross, G. Gordon, and D. Bagnell, "A reduction of imitation learning and structured prediction to No-Regret online learning," in *International Conference on Artificial Intelligence and Statistics*, ser. Proceedings of Machine Learning Research, G. Gordon, D. Dunson, and M. Dudík, Eds., vol. 15. Fort Lauderdale, FL, USA: PMLR, 2011.
- [27] D. Chen, B. Zhou, V. Koltun, and P. Krähenbühl, "Learning by cheating," in *Conference on Robot Learning (CoRL)*, 2019.
- [28] P. A. Ortega, M. Kunesch, G. Delétang, T. Genewein, J. Grau-Moya, J. Veness, J. Buchli, J. Degraeve, B. Piot, J. Perolat, T. Everitt, C. Tallec, E. Parisotto, T. Erez, Y. Chen, S. Reed, M. Hutter, N. de Freitas, and S. Legg, "Shaking the foundations: delusions in sequence models for interaction and control," Oct. 2021.
- [29] G. Swamy, S. Choudhury, J. A. Bagnell, and Z. S. Wu, "Sequence model imitation learning with unobserved contexts," *Advances in Neural Information Processing Systems*, vol. 35, 2022.
- [30] R. Vuorio, P. D. Haan, J. Brehmer, H. Ackermann, D. Dijkman, and T. Cohen, "Deconfounding imitation learning with variational inference," *Transactions on Machine Learning Research*, 2024, expert Certification. [Online]. Available: <https://openreview.net/forum?id=3FsVtsISHW>
- [31] B. Wilson, W. Qi, T. Agarwal, J. Lambert, J. Singh, S. Khandelwal, B. Pan, R. Kumar, A. Hartnett, J. K. Pontes, et al., "Argoverse 2: Next generation datasets for self-driving perception and forecasting," *arXiv preprint arXiv:2301.00493*, 2023.
- [32] H. Caesar, J. Kabzan, K. S. Tan, W. K. Fong, E. Wolff, A. Lang, L. Fletcher, O. Beijbom, and S. Omari, "nuplan: A closed-loop ml-based planning benchmark for autonomous vehicles," *arXiv preprint arXiv:2106.11810*, 2021.
- [33] E. Vinitzky, N. Lichtlé, X. Yang, B. Amos, and J. Foerster, "Nocturne: a scalable driving benchmark for bringing multi-agent learning one step closer to the real world," 2023. [Online]. Available: <https://arxiv.org/abs/2206.09889>
- [34] N. Montali, J. Lambert, P. Mouglin, A. Kuefler, N. Rhinehart, M. Li, C. Gulino, T. Emrich, Z. Yang, S. Whiteson, B. White, and D. Anguelov, "The waymo open sim agents challenge," in *Advances in Neural Information Processing Systems*, A. Oh, T. Naumann, A. Globerson, K. Saenko, M. Hardt, and S. Levine, Eds., vol. 36. Curran Associates, Inc., 2023, pp. 59 151–59 171. [Online]. Available: https://proceedings.neurips.cc/paper_files/paper/2023/file/b96ce67b2f2d45e4b315e13a6b5b9c5-Paper-Datasets_and_Benchmarks.pdf
- [35] W. Wu, X. Feng, Z. Gao, and Y. Kan, "Smart: Scalable multi-agent real-time simulation via next-token prediction," *arXiv preprint arXiv:2405.15677*, 2024.